Section A -Research paper

Synthesis, characterisation and pharmacological studies of ferrous (II), cobalt (II), nickel (II), palladium (II), manganese (II) and copper (II) complexes of pyrrolo pyrimidine derivatives

Abhay Bagul[a], Digamber Gaikwad[a*], Yogesh Patil[b] and Nilesh Bhusari[c]

Article History: Received: 02.05.2023 **Revised:** 20.06.2023 **Accepted:** 28.06.2023

Abstract

The structure's M (II) complexes [ML_2] have been synthesized using a Schiff base from 4-chlorobenzaldehyde and pyrrolopyrimidinehydrazide. According to the metal content analysis, a new series of Fe(II), Pd(III), Mn(II), Co(II), Ni(II), Cu(II), and Mn(II) metal complexes are created with a 2:1 ligand: metal ratio. The metallic ion is coordinated by nitrogen atoms from the azomethine, pyrrolo, and pyrimidine rings. The Fourier Transform-Infra Red (FT-IR), Ultraviolet-Visible Spectra (UV-Vis Spectra), 1H-Proton, and 13-Carbon Nuclear Magnetic Resonance (for the ligand), ESR, Magnetic Susceptibility at 25 °C, and Conductivity measurements have all been used to infer the stereochemistry of the ligand complexes. The conductivity measurements demonstrate the metal complexes' non-electrolytic behavior. Notwithstanding the possible exception of the Pd(II) complex, which has a square planar geometric structure, electronic spectra analysis research demonstrated that all complexes have an octahedral structure. Magnetic moment and conductance studies supported this research. The Minimum Inhibitory Concentration approach was used to test the antibacterial and antifungal effects of the Schiff bases and their metal complexes on *Escherichia coli, Staphylococcus aureus, Pseudomonas aeruginosa*, and *B. subtilis*.

Keywords: Schiff base ligand, Ultraviolet-Visible Spectra, Metal complex and 4-chlorobenzaldehyde

[a]Department of Forensic Chemistry, Government Institute of Forensic Sciences,
Aurangabad 431004, Maharashtra, India, *Corresponding Author : gaikwad.dd.dg@gmail.com
[b]Department of Chemistry, Vasantrao Naik Mahavidhyalaya, Aurangabad 431003, Maharashtra, India,
[c] Department of Forensic Chemistry, Government Institute of Forensic Science, Aurangabad, India

DOI: 10.48047/ecb/2023.12.si7.123

Introduction

Organic interactions involving the condensation of two or more types of molecules to obtain a new derived from imine compounds as a commonly used compound for this purpose are necessary for designing drugs from organic compounds with new and practically important biological behaviours [1-4]. An important product is produced when primary amines are condensed with aldehydes or ketones. The Schiff base reaction was conducted as usual. Due to the stability of complexes of metal ions in various oxidation states, as well as its extensive involvement in biological processes and other important large-scale processes like industrial fields and as catalysts for reactions, the presence of a Schiff base in our interactions is crucial [5]. The nitrogen lone pair electrons on azomethine (-N=CH) bonding are thought to be responsible for the stable structure of metal complexes [6]. Through binding to metal ions, donor atoms of Schiff base ligands can increase their antibacterial activity [7-9]. Metal ions can interact with Schiff base ligands to form structures with various geometrical shapes. These structures can be used in various ways, including designing significant medicinal compounds and developing anti-tumour, anti-cancer, anti-bacterial, anti-viral, and anti-fungal compounds in the geology field [10, 11]. In forming transition metal complexes, the influence of pH and concentrations of tetradentate donor ligands of type N_2O_2 has been investigated [12]. Oxalic Acid with Schiff base trimethoprim chelates and β-enaminone with 8-hydroxyquinoline play significant roles in biological processes such as activating transport molecules across membranes, storage, and enzymes [13, 14].

Pyrrolopyrimidine-derived ligands have a wide range of uses in industry, pharmaceuticals, synthetic resins, polymers, agrochemicals, antiseptic agents, and insecticides, as well as in Barmastine and an anti-hepatitis-B drug [15, 16]. In this study, a novel Schiff base ligand called 4-[(2E)-2-(4-chlorobenzylidene)hydrazinyl]-7H-pyrrolo[2,3-d]pyrimidine was synthesised, described, and subjected to antimicrobial studies and its metal complexes with Fe(II), Pd(II), Mn(II), Co(II), Ni(II), and Cu(II).

Materials and Methods:

All chemical reagents used were of the highest purity and analytical quality from (BDH). All organic solvents are spectroscopically pure from (S. d. fine), including ethanol, MDC, and dimethylsulfoxide (DMSO).

Instruments:

TMS was the internal standard for BRUKER AVANCE III HD NMR 500 MHz PMR spectra

in DMSO-d_6 at room temperature. BRUKER FT-IR spectrophotometers measured 4000-500 cm^{-1} KBr pellet spectra. Chemical elements were analysed using the Carlo-Erba LA-118 microdosimetry to count C, H, N, and Cl concentrations. Gouy's method [17] tested solid compounds' magnetic susceptibility. The conductivity measurement experiment used 10^{-3} M HPLC-grade nitrobenzene solutions at room temperature.

Synthesis of ligand 4-[(2E)-2-(4-chlorobenzylidene)hydrazinyl]-7H-pyrrolo[2,3-d]pyrimidine (HPPH*p*CB):

A conical flask with a capacity of 250 mL was used for keeping 14.06 g (0.1 mol) of *p*-chlorobenzaldehyde. After adding 50 mL of 100% ethanol to the mixture, it was stirred for 10 minutes. Following the addition of three drops of concentrated HCl, the mixture was stirred for 10 minutes before the addition of (14.90 g, 0.1 mol) of 4-hydrazinyl-7H-pyrrolo[2,3-d] pyrimidine dissolved in 100% ethanol (25 ml). The solution was cooled after being refluxed and agitated at 70–80 °C for five hours, during which the reaction was observed using the TLC technique (Rf = 0.84). The precipitate was then filtered and allowed to dry, producing a pale-yellow precipitate, which was then recrystallized using hot ethanol.

Synthesis of (L-FSB) metal complexes:

Synthesis of [Fe(PPH*p*CB)$_2$] complex:

Ferrous sulphate ($FeSO_4$) (0.759 g, 0.5 mmol) was dissolved in 5 mL of distilled water before being added gradually to the mixture of HPPH*p*CB ligand (2.71 g, 1.0 mmol) in 20 mL of ethanol. The mixture was stirred for 30 minutes; pH was adjusted to 7 by 0.1N NaOH, followed by 3 hours of refluxing at 70 to 80 °C. The solution was then allowed to cool and create a violet precipitate, which was then collected and recrystallized with hot ethanol to produce a dark violet precipitate.

Synthesis of [M(PPH*p*CB)$_2$] complexes:

For the preparation of metal complexes, a similar interaction was utilized as in the past: metal buildings using (1 mmol) of metal particle salts: (0.237 g, $CoCl_2.6H_2O$), (0.197.93 g, $MnCl_2.4H_2O$), (0.237 g, $NiCl_2.6H_2O$), (0.170 g, $CuCl_2.2H_2O$), and (0.18 g, $PdCl_2$) with (2 mmol) of the ligand (0.54 g, (HPPH*p*CB) to give various shades of edifices encourages which were gathered by filtration, washed with ethanol, and afterwards, vacuum dried.

Biological activities:

Method of preparation of agricultural media:

The nutritional media (Muller Hinton agar) was made by dissolving a gram of powder in a litre of distilled water (pH = 7.3) and then sterilising it with Auto Cleave. This medium was used to cultivate microorganisms and investigate the antagonistic activity of compounds against the isolates utilised in this investigation.

Preparation of microorganism suspension:

Colonies of each of the microorganisms under study were taken and diluted to a concentration of 0.85% in sterile physiological saline to create the suspension of bacteria. The Petridis dishes assessed the biological activity against the investigated chemical substances in their production.

Microorganisms testing the inhibitory activity of complexes in facultative

By introducing 20–25 mL of agar medium to each plate and keeping them in the incubator for a full day (1 h) at 37 °C to avoid dish contamination, the agar well diffusion method was used to observe the impact of the study's ligands and chemical complexes on the growth of microorganisms. A hole was drilled in the surface of the culture medium using a glass spreader, and 10 mL of the prepared microorganism suspension, which contained 1.5810 cells/mm as described in the preceding sentence, was then spread uniformly on the surface of the agar media. The plates were placed in the refrigerated for 30 minutes at 4 °C, then incubated in the incubator at 37 °C with 100 micro ml of chemical complexes for each well at a concentration of $1x10^{-3}$ M, with the remaining solvent (DMSO) placed in the control hole.

Results and Discussion

Synthesis and physical properties of HPPH*p*CB ligand and Its metal complexes

The condensation reaction of *p*-chlorobenzaldehyde with 4-hydrazinyl-7H-pyrrolo[2,3-d] pyrimidine in a mole ratio (1:1), respectively, produced the novel Schiff base HPPH*p*CB, which is a derivative of 4-hydrazinyl-7H-pyrrolo[2,3-*d*] pyrimidine. **Scheme 1** illustrates the reaction. Melting point, TLC, FT-IR, UV-Vis, ^{1}H-NMR, and mass ESR data were used to characterise and validate the synthesis of the HPPH*p*CB ligand. It was discovered to be airborne stability. This ligand was barely soluble in water but in DMSO, DMF, and THF diethyl ether, methanol, ethanol, acetone,

chloroform, ethyl acetate, and benzene. It has been investigated how synthesised (HPPH*p*CB) ligands interact with their metal ions, including Fe(II), Co(II), Mn(II), Ni(II), Cu(II), and Pd(II). According to analytical data on the metal content of the ligand (HPPH*p*CB) and its metal complexes, the metal-to-ligand ratio was (1:2). Most complexes exhibit stability and have high melting points. **Table 1** lists the physical characteristics of the ligand (HPPH*p*CB) and its complexes. At 301K (in 10^{-3}M nitrobenzene), the complexes have molar conductance values between 0.351 - 5.863 Ω^{-1} cm^2 mol^{-1}, making them non-electrolytes.

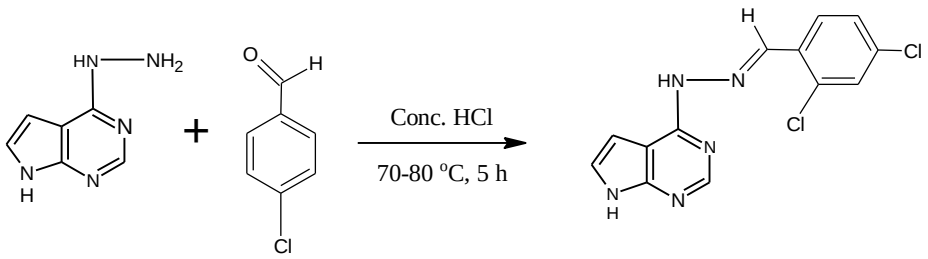

Scheme 1: Condensation reaction between *p*-chlorobenzaldehyde and 4-hydrazinyl-7H-pyrrolo[2,3-d] pyrimidine

Table 1: Physical properties of ligand (HPPH*p*CB) and its complexes

Comp	Colour	MW	% Yield	MP/DP	Element Content					Cond	MM
					M	C	H	N	Cl		
HPPH*p*CB	L. Brown	271.000	81.47	187	-	57.49	3.71	25.78	13.05	-	-
Mn(PPH*p*CB)$_2$	White	594.938	82.45	205	9.23	52.44	3.03	23.53	11.93	3.075	-
Fe(PPH*p*CB)$_2$	Blue	595.845	80.09	209	9.37	52.36	3.02	23.5	11.91	1.734	5.23
Co(PPH*p*CB)$_2$	Brown	598.993	81.55	214	9.85	52.09	3.01	23.37	11.90	1.574	5.02
Ni(PPH*p*CB)$_2$	Green	598.693	71.99	208	9.8	52.11	3.01	23.38	11.90	1.102	3.01
Pd(PPH*p*CB)$_2$	Brown	646.000	82.32	215	16.41	48.30	2.79	21.67	17.00	0.341	-
Cu(PPH*p*CB)$_2$	Green	603.000	75.68	208	10.5	51.69	2.98	23.2	11.80	5.863	1.86

Spectroscopy studies

FT-IR spectra of the ligand (HPPH*p*CB):

Due to the formation of azomethine, the newly developed ligand (HPPH*p*CB)'s FT-IR spectra showed a sharp, divided, and new band at 1630 and 1624 cm^{-1}. (>CH=N) is a sign that the 4-hydrazinyl-7H-pyrrolo[2,3-d] pyrimidine compound's amino group (NH_2) condensed with the *p*-chlorobenzaldehyde aldehyde group to form the azomethine group [18].

FT-IR spectra of ligand (HPPH*p*CB) and its metal complexes:

The band at 1584 cm^{-1} that is attributed to azomethine in the infrared spectra of the free ligand (HPPH*p*CB), **Figure 1**, was moved to a lower frequency by 9-13 cm^{-1} in all complexes, showing that azomethine's nitrogen atoms were involved in the coordination of complexes [19]. Due to the presence of the NH group of the pyrrolo ring, the ligand (HPPH*p*CB) displayed broadband at

3290 cm^{-1}; this band was absent in all produced metal complexes, indicating that this NH group was deprotonated during complexation. However, because (M-N) confirmed the coordinated behaviour of (HPPH*p*CB) was monodentate through the coordinate by nitrogen atom of the azomethine group [20], all complexes displayed new bands in the 506-523 cm^{-1} region. **Table 2** displays the ligand's (HPPH*p*CB) and its metal complexes' notable absorption bands.

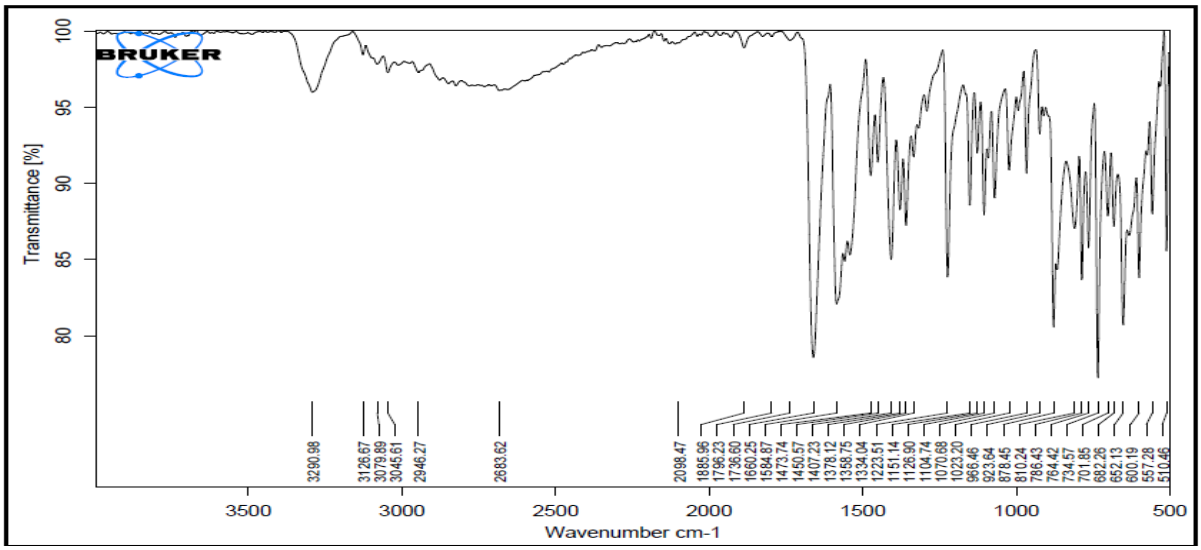

Figure 1: FT(IR) spectrum of HPPH*p*CB ligand

Table-2: FT(IR) spectral data of HPPH*p*CB ligand and its metal complexes

Comp	NH (Ali)	NH (Aro)	C-H (Aro)	C-H (aldehyde)	>C=N- (aro)	>C=N- (Ali)	C-N (aro amine)	C-Cl	o—di sub benzene ring	M-N/M→N
HPPH*p*CB	3290	3126	3060	2946	2883	1584	1312	926	734	-
Mn(PPH*p*CB)$_2$	3377	-	3053	2974	2834	1576	1307	919	724	521, 509
Fe(PPH*p*CB)$_2$	3195	-	3065	2981	2835	1575	1308	919	726	526, 507
Co(PPH*p*CB)$_2$	3402	-	3064	2979	2836	1574	1307	918	725	522, 506
Ni(PPH*p*CB)$_2$	3195	-	3065	2980	2836	1575	1308	919	724	523, 507
Pd(PPH*p*CB)$_2$	3291	-	3049	2930	2824	1572	1334	925	735	527, 510
Cu(PPH*p*CB)$_2$	3348	-	3050	2978	2833	1571	1306	920	724	523, 506

^{1}H-NMR of the ligand (HPPH*p*CB):

The ^{1}H-NMR spectra of the ligand (HPPH*p*CB), **Figure 2**, showed one signal at δ = 12.99 ppm due to one proton of aromatic NH of the pyrrole ring; this signal disappeared in Pd(II) complex, indicating that this amine group deprotonated during complexation [21], and multiplet signals at δ = 7.24-8.50 ppm due to 7 protons of aromatic ring. The azomethine group's H proton generates the singlet signal at δ = 8.72ppm. Finally, the -CH= group is accountable for the chemical shift at δ = 8.77 ppm [22].

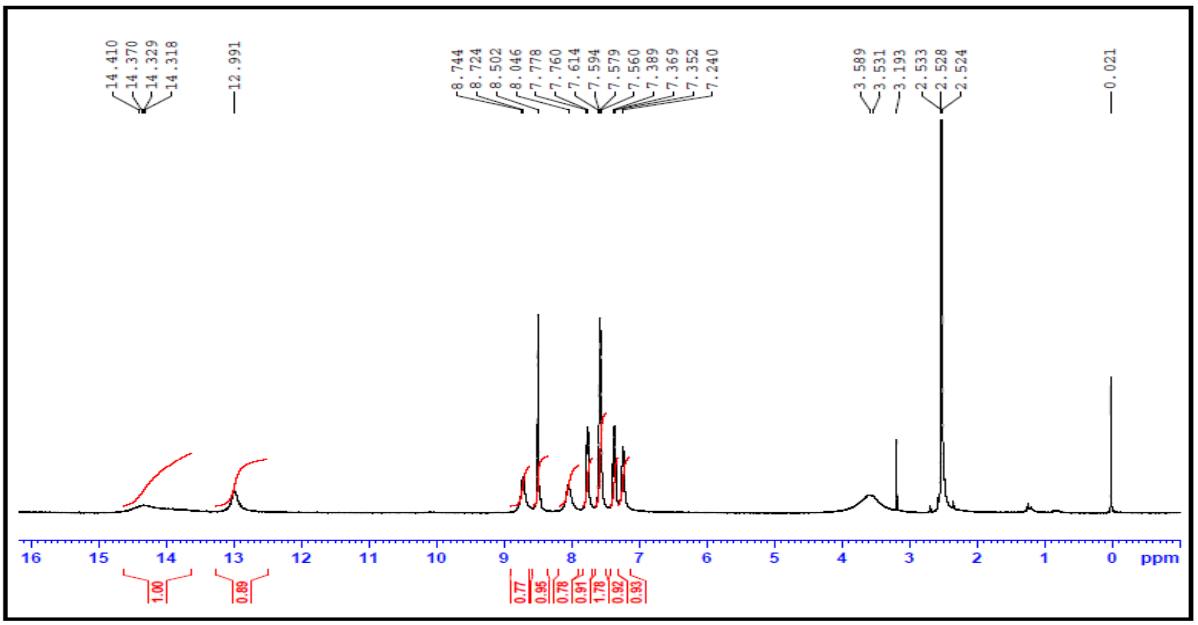

Figure 2: ^{1}H NMR spectrum of HPPH*p*CB ligand

Table-3: ^{1}H NMR spectral data of HPPH*p*CB ligand and its metal complexes

Comp	NH (aro)	CH (Ali)	NH (Ali)	Aromatic Protons
HPPH*p*CB	12.99	8.77	8.72	7.24-8.50
Pd(PPH*p*CB)$_2$	-	8.75	8.72	7.23-8.50

^{13}C-NMR of the ligand (HPPH*p*CB):

The spectrum analysis of ^{13}C-NMR for the produced ligand using DMSO-d_6 is shown in **Figure 3**, with the signal at δ = 17.54 ppm assigned to the carbon atom of which methyl group. Multiple signals at positions δ = 121.15, 123.98, 129.75, 132.42, and 134.8 ppm due to aromatic ring carbon atoms, and the spectrum also displays multiple signals at positions δ = 112.36, 118.46, 147.08, and 150.03 ppm due to furan ring carbon atoms. The azomethine group's carbon atom signal point developed at δ = 145.53 ppm [22].

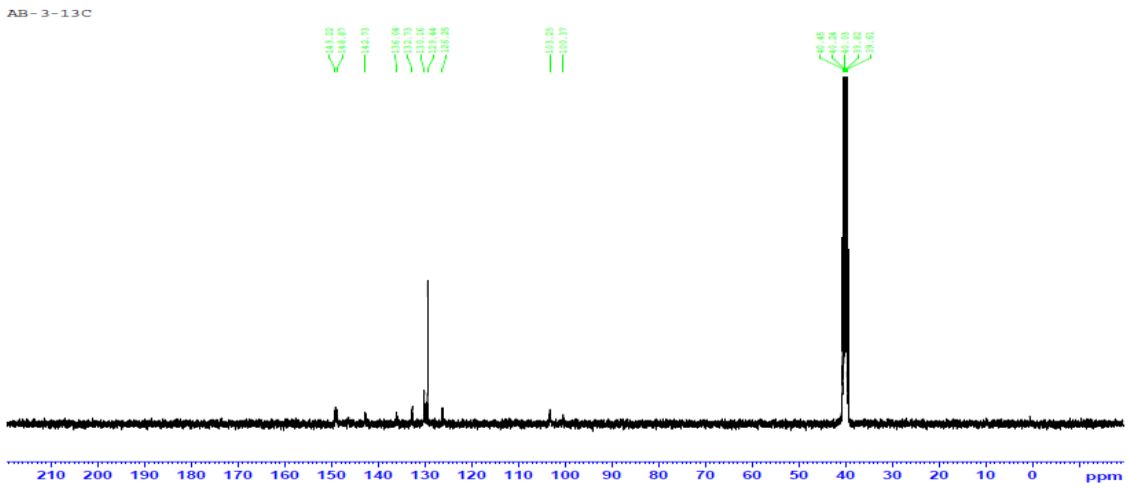

Figure 3: ^{13}C NMR spectrum of HPPH*p*CB ligand

Table-4: ^{13}C NMR spectral data of HPPH*p*CB ligand

Comp	-CH=	CH methyl group	Aromatic carbon				
HPPH*p*CB	145.53	17.54	121.15	123.98	129.75	132.42	134.8

UV-spectra of the ligand (HPPH*p*CB):

The UV-Vis spectra of pale yellow HPPH*p*CB in DMSO, Figure 6 solvent, showed two absorption bands with high intensity at 273 nm and 319 nm, which are assigned to $\pi\rightarrow\pi^*$ and $n\rightarrow\pi^*$ for electronic transitions of aromatic or pyrrole ring and azomethine group, respectively [23].

The UV-Vis spectrum of the metal complex:

The ligand field or charge transfer band was responsible for all the complexes' greater intensity absorption bands in the UV range. The UV-Vis spectrum of the pale brown manganese (II) complex revealed an absorption band at 352 nm and a charge transfer band at 284 nm. The magnetic susceptibility of the manganese (II) solid complex was measured at 5.49 BM at room temperature, which is due to the presence of five individual electrons with a high spin state, and this is supported by the measurements value of molar conductivity in DMSO solvent was non-electrolyte in addition to these results, FT(IR), and metal content [24].

Based on magnetic susceptibility tests, the [Fe(PPH*p*CB)$_2$] complex is paramagnetic at 301K, confirming its 2+ iron oxidation state. The $^5T_{2g}\rightarrow{}^5E_g$ transition [25] was attributed to the electronic spectra of the Fe(II) complex, showing an absorption band at 666 nm. Furthermore, the L → M charge transfer band is at 418 and 235 nm. According to high spin octahedral geometry [26-29], the magnetic moment of the [Fe(PPH*p*CB)$_2$] complex was 5.23 B.M. At 301K, the magnetic moment of the [Fe(PPH*p*CB)$_2$] complex is 5.23 BM. Octahedral Fe(II) complexes have been reported to have values that are in good accord with this one. Two absorptions, one at 900 nm assigned to $^4T_{1g}(F)\rightarrow{}^4T_{2g}(F)$ (ν_1) and the other at 515 nm assigned to $^4T_{1g}(F)\rightarrow{}^4T_{2g}(P)$ (ν_2), were observed for the [Fe(PPH*p*CB)$_2$] complex, indicating an octahedral geometry surrounding the Fe(II) ion [30].

The brown Cobalt(II) complex's UV-vis spectra show two absorption bands at 910 and 783 nm, respectively. These bands are seen in the visible region's fundamental at 783 nm; the transition may be responsible for it. $^4T_{1g}$ (F) → $^4T_{1g}$(F) (υ_2), the other electronic transition bands type $^4T_{1g}$(F) → $^4T_{2g}$(F) (υ_1) and $^4T_{1g}$ → $^4T_{1g}$(P) (υ_3) could not be detected or is very weak, so besides studying magnetic moments at room temperature of Co(II) complex was (5.02 B.M) confirmed high spin of d^7 ion and that indicate the paramagnetic nature. Molar conductivity in nitrobenzene was measured to be non-electrolyte. These findings, along with those from FT(IR) and metal content, led us to propose the Co(II) complex's octahedral geometry [31].

The green nickel (II) complex's UV-Vis spectrum reveals an electronic transition band with

high intensity at 475 nm, which is attributed to (*d-d*) electronic transition type $^3A_{2g} \rightarrow {}^3T_{1g}(P)$. In contrast, the other two electronic transition bands, $^3A_{2g} \rightarrow {}^3T_{1g}(F)$ and $^3A_{1g} \rightarrow {}^3T_{2g}(F)$ were either not detectable or weakly present. In addition to these results, FT-IR, and metal content, we proposed the distorted octahedral geometry of the Ni(II) complex. The magnetic moment measurement of the nickel (II) solid complex showed a value of 3.01 B.M at room temperature due to two individual electrons with high spin states. This is supported by the measurements value of molar conductivity in nitrobenzene solvent was non-electrolyte.

The electronic transition type ($^2B_{1g} \rightarrow {}^2B_{2g}$) can be identified in the UV-Vis spectra of a dark green Copper (II) complex that exhibits a weak intensity adsorption band at 640 nm. We proposed the distorted octahedral geometry of the Cu(II) complex based on these findings, which showed that the magnetic moment value of the solid Cu(II) is 1.86 B.M. at room temperature and was also confirmed by the results of molar conductivity in nitrobenzene solvent is non-electrolyte [32, 33]. Palladium (II) complex, a dark brown colour, UV-Vis spectrum, the charge transfer spectrum of the Pd(II) complex is responsible for the presence of a tail that reaches a wavelength of around 425 nm. Due to the diamagnetic nature of the Pd(II) complex and its non-electrolyte molar conductance, along with the results of the FT(IR) and metal content, we proposed the square planar geometry of Pd(II) [34]. **Table 1** contains results for complexes' molar conductance, magnetic moment, and UV-Vis Spectra.

Electron paramagnetic resonance (EPR) spectrum of Cu(II) complex:

Electron Spin Resonance (ESR), also identified as Electron Paramagnetic Resonance (EPR) spectroscopy, is the instrumental technique which involves microwave-induced resonance transitions between the magnetic energy levels of the electron that possess a net spin moment. It can be used to investigate the paramagnetic species with one or many spin-free electrons, viz., free radicals, diradicals, metal coordination compounds with paramagnetic metal centres, defects in semiconductors, irradiation effects in solids, etc. ESR spectra of [Cu(PPH*p*CB)$_2$] is recorded at LNT in chloroform solution, on X-band at 9.1 GHz in the magnetic field of 0.3 T. Interpretation of the ESR spectra of the above said complex gives the following values $g_\perp$ = 1.9806, $g_{||}$ = 1.8449, g_{ave} = 1.9128.

Calculations of ESR parameters:

$g_\perp$	$g_{\|\|}$	g_{ave}
1.9806	1.8449	1.9128

The electronic paramagnetic resonance (EPR) experiments on the Cu(II) complex of HPPH*p*CB in

the polycrystalline form at liquid nitrogen temperature (LNT) on the X-band at 9.1 GHz. under the magnetic field of 0.3 T were attempted to obtain analytical information on the type of bonding in this complex. The room temperature spectrum of the [Cu(PPH*p*CB)$_2$] was poorly resolved, with the LNT spectrum showing only slightly improved resolution. The low resolution of the spectrum is due to the low crystallinity of the complex[26]. The nature of the EPR spectrum of this complex suggests a distorted octahedral structure[27] as the two g values follow the trend $g_{\perp} > g_{||}$ suggesting that the coordination compound is tetragonally compressed at ambient temperature. The g tensors were evaluated based on Kneubuhl's analysis. Hathaway *et al.* has shown that a factor G which is $g_{||}$-2/$g_{\perp}$-2 can give important information on whether the observed $g_{||}$ and $g_{\perp}$ values suggest the local Cu(II) environment. Their resonating was that since Kneubuhl's method ignores hyperfine coupling constants, the absolute g-values are possibly in error and, further, that the components that affect the correlation between the g value of the local Cu(II) environment and the g values of the bulk true solid, may be measured with the interaction between the remote Cu(II) ions in a non-dilute magnetic system. The authors also proposed that, if exchange coupling interaction is larger than heat energy, imperfect spin-pairing may result. However, when the scene magnetic values that is higher than the spin-only moments then the coupling exchange interaction, whenever occurs, must have its energy lower than the heat energy. Then, such interactions influence the line shapes and do not reduce the magnetic moments below the spin-only values. When the exchange interactions take up the value that is in between the equivalent ions crystallographically, then the sharp absorption lines appear and the obtained 'g' values gives the local 'g' values. If the interaction is among the non-equivalent crystallographically ion then it results in notable broadening of spectrum may occur and an isotropic spectrum would result. However, if the interaction is among the non-crystallographically equivalent ions then the observed $g_{\perp}$ could be greater than the local $g_{\perp}$. At the same time, the $g_{||}$value could be similar than the local $g_{||}$ values. This would be reflected in the values of G being ≥ 4. Therefore, values of $G > 4$ indicate absence of exchange coupling. In the cupric complexes of HPPH*p*CB ligand, the high G values found may imply negligible exchange interactions.

Antimicrobial activity studies:

Using the disk diffusion method, the newly synthesised pyrrolopyrimidine-based Schiff base ligand (HPPH*p*CB) and their metal complexes were tested for their antimicrobial properties against six pathogenic bacterial Gram-negative (*P. aureginosa* and *E. coli*), Gram-positive (*B. substilis* and *S. aureus*), and fungi (*Candida albicans* and *saccharomyces cerevisiae*) strains. To create a solution with a concentration of 10 mg/mL, the test (HPPH*p*CB) ligand and metal complexes were dissolved in (DMSO) [35, 36]. The prepared ligand (HPPH*p*CB) and its complexes have antibacterial and

antifungal properties. With the same dosage, the synthesised ligand (HPPH*p*CB) inhibited both positive and negative microorganisms. Gram-positive and Gram-negative bacteria were active against it in varying degrees in all derivate complexes. While the complex of Palladium (II) and Nickel (II) showed better inhibitory activity than the other complexes against the bacteria *E. coli*, the Palladium (II) and Cobalt (II) complex is more effective than other complexes against bacteria (*Staphylococcus aureus*). Compared to its activity against bacteria, the synthesised ligand (LFSB) demonstrated high inhibitory activity against Candida albicans with the ability of all complexes produced from it. At varied ratios, copper (II) and palladium (II) complexes had better inhibitory effects against fungi than the other complexes. The prepared ligand and its complexes are efficient against *E. coli* and staph germs for several reasons, including:

1. The fatty layer of these bacteria's cell walls can be broken down by the solutions of these ligands and their complexes, resulting in the liquid inside the cell leaking out and killing the bacteria.

2- The prepared ligand's (LFSB) ability to form complexes with the metallic elements present in cells, such as magnesium, zinc, calcium, copper, cobalt, and iron, deprives bacteria of these vital components and renders them incapable of committing self-harm [37, 38].

Conclusion:

Based on the results of metal content, a new Schiff base made from 4-hydrazinyl-7H-pyrrolo[2,3-*d*] pyrimidine has been coordinated with a new series of metal complexes of Fe(II), Mn(II), Co(II), Ni(II), Cu(II), and Pd(II). The ratio of metal to ligand is 1 to 2. The FT(IR), UV-Vis, ^{1}H, ^{13}C NMR, ESR spectra, magnetic moment, and molar conductivity are used to characterize these compounds. The metal coordination between the azomethine and pyrrolopyrimidine rings is explained by FT-IR. The ligand's (HPPH*p*CB) FT-IR results and those from the ^{1}H-NMR and ^{13}C-NMR spectra agreed. Conductance experiments revealed that all complexes of Fe(II), Mn(II), Co(II), Ni(II), Cu(II), and Pd(II) are non-electrolytes. The octahedral geometrical structure of all complexes, except the Pd(II) complex, is confirmed by the analysis of UV-Visible spectra and magnetic moment measurements. To comprehend the impact of binding metal ions to the (HPPH*p*CB) ligand, the biological analysis of (HPPH*p*CB) and its complexes against Gram-negative (*P. aureginosa* and *E. coli*), Gram-positive (*B. substilis* and *S. aureu*s), and Candida albicans bacteria were examined. According to an antimicrobial investigation, metal complexes exhibit more inhibition than the (HPPH*p*CB) ligand. On the basis of spectral data, structure of the transition metal complexes assigned as;

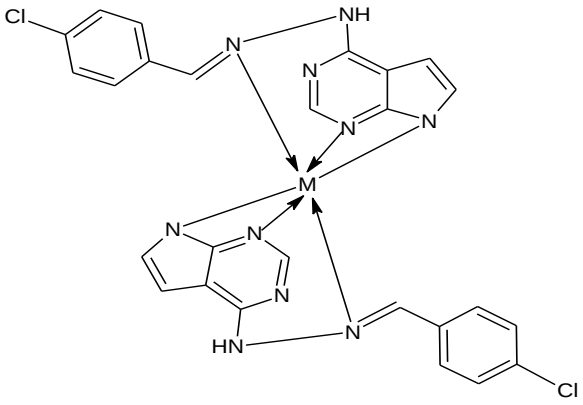

References:

1. Manivel S., Gangadharappa B.S., Elangovan N., Thomas R., Abu Ali O.A., Saleh D., *Journal of Molecular Liquids*, **2022**, 350:118531.
2. EI–Sonbati A.Z., Mahmoud W.H., Mohamed G.G., Diab M.A., Morgan S.M., Abbas S.Y., *Applied Organometallic Chemistry*, **2019**, 33:e5048.
3. Badeea Y.A., Mahdi W.K., Ibrahim Y., Musa F.H., Synthesis, *International Journal of Drug Delivery Technology*, **2021**, 11:735.
4. Tahar T.A., Mahdi W.K., Musa F.H., *Journal for Pure and Applied Sciences*, **2017**, 30:77.
5. De S., Jain A., Dr. Barman P., *Chemistry Select review*, **2022**, 7:e202104334.
6. Nashaan F.A., Al-Rawi M.S., *Chemical Methodologies*, **2023**, 7:106.
7. Al-Redha H.M.A., Ali S.H., Mohammed S.S., *Baghdad Science Journal*, **2022**, 19:704.
8. Sahib S.K., Abdul Karem L.K., *Baghdad Science Journal*, **2020**, 17:99.
9. Al-Hamdani A.A.S., Shaalan N.D., Bakir S.R., *Baghdad Science Journal*, **2015**, 12:350.
10. Kumar S.M.,Rajesh J.,Anitha K., Dhahagani K., Marappan M., Gandhi N.I., Rajagopal G., *Spectrochimica Acta Part A: Molecular and Biomolecular Spectroscopy*, **2015**, 142:292.
11. Pahonţu E., Julea F., Chumakov Y., Petrenco P., Roşu T., Gulea A., *Journal of Organometallic Chemistry*, **2017**, 836- 837:40.
12. Dawood J.I.J., Mahdi W.K., Al-Shemary R.K.R., *Research Journal of Pharmacy and Technology*, **2019**, 12:4471.
13. M.B. Abdulsalami, Numani A.T., *Chemical Methodologies*, **2022**, 6:962.
14. Abdalrazaq E., Jbarah A.A.Q., Al-Noor T.H., Shinain G.T., Jawad M.M., *Indonesian Journal of Chemistry.*, **2022**, 22:1348.
15. Khalil OM, Kamal AM, Bua S, Teba HE, Nissan YM, Supuran CT, *European*

Journal of Medicinal Chemistry, **2020**, 188:112021.

16. McCarty RM, Bandarian V, *Bioorganic chemistry*, **2012**, 1;43:15-25.
17. Dutta RL, Syamal A. Elements of magnetochemistry. Affiliated East-West Press; **1993**.
18. Alturiqi A.S., Alaghaz A.N., Ammar R.A., Zayed M.E., *Journal of Chemistry*, **2018**, 2018:5816906.
19. Nashaan F.A., Al-Raw M.S., *Chemical Methodology*, **2023**, 7:267.
20. Sumathi R.B., Halli M.B., *Bioinorganic Chemistry and Applications*, **2014**, 2014:942162.
21. Ahmed T.T., Alajrawy O.I., *Materials Today: Proceedings*, **2021.**
22. Larial F.Y., El-Barasi M.M., Maihub A.A., Mohapatra R.K., Al–Noor T.H., *Academic Journal of Chem. Methodol.*, **2023**, 7(6) 419-434 433.
23. Saeed S.E.S., Al-Harbi T.M., Alhakimi A.N., Abd El-Hady M.M., *Coatings*, **2022**, 12:1181.
24. Meenukutty M.S., Mohan A.P., Vidya V.G., Viju Kumar V.G., *Heliyon*, **2022**, 8:e09600.
25. Suresh M.S., Prakash V., *E-Journal of Chemistry*, **2011**, 8:1408.
26. Van Kuiken B. E., Hahn A. W., Nayyar B., Schiewer C. E., Lee S. C., Meyer F. and DeBeer S., *Inorg. Chem*., **2018**, 57:12 7355.
27. Tarrago M., Römelt C., Nehrkorn J., Schnegg A., Neese, Bill E. and Ye S., *Inorg. Chem.*, **2021**, 60:7, 4966.
28. Badekar R.R., Kulkarni S.W., Lokhande R.S. and Thawkar B.S., *Int. J. of Applied Res.*, **2016**, 2(9):175.
29. Mohamed G., *Spectrochimica Acta Part A: Molecular and Biomolecular Spectroscopy*, **2001**, 57:8, 1643.
30. Al-Omair M. A., *Arabian J. of Chem*., **2018**.
31. Mohapatra R.K., Mishra U.K., Mishra S.K., Mahapatra A., Dash D.C., *Journal of the Korean Chemical Society*, **2011**, 55:926.
32. Khalaji A.D., Rad S.M., Grivani G., Das D., *Journal of Thermal Analysis and Calorimetry*, **2011**, 103:747.
33. Singh K., Barwa M.S., Tyagi P., *European Journal of Medicinal Chemistry*, **2007**, 42:394.
34. Saghatforoush L.A., Aminkhani A., Ershad S., Karimnezhad G., Ghammamy S., Kabiri R., *Molecules*, **2008**, 13:804.
35. Sumrra S.H., Ibrahim M., Ambreen S., Imran M., Danish M., Rehmani F.S,

Bioinorganic Chemistry and Applications, **2014**, 2014:812924.

36. Diab M.A., El-Sonbati A.Z., Morgan S.M., ElMogazy M.A., Applied Organometallic Chemistry, **2018**, 32:e4378.
37. Ismail B., Nassara D.A., El–Wahabb Z.A., Ali O.A.M., *Journal of Molecular Structure*, **2021**, 1227:129393.
38. Mohamed G.G., Zayed E.M., Hindy A.M.M., *Spectrochimica Acta part A: Molecular and Biomolecular spectroscopy*, **2015**, 145:76.